Transitions from large to small ELMs and to edge turbulence with no ELMs

BOUT++
Boundary Plasma Turbulence Code

X.Q.Xu[1], T.Y.Xia[1,2], C. H. Ma[1,3], B.Gui[1,2], P.W.Xi[1,3], A.Dimits[1], I.Joseph[1], M.V.Umansky[1], S.S.Kim[4], T.Rhee[4], G.Y.Park[4], H.Jhang[4], P.H.Diamond[4,5], B.Dudson[6], P.B.Snyder[7]

[1]LLNL, [2]ASIPP, [3]PKU, [4]NFRI,[5]UCSD,[6]U.York,[7]GA

Presented at
24th Pedestal and Edge Topical Group Meeting
April 22, 2013, Garching, Germany

This work was performed under the auspices of the U.S. DoE by LLNL under Contract DE-AC52-07NA27344 and is supported by the China NSF under Contract No.10721505, the National Magnetic Confinement Fusion Science Program of China under Contracts No. 2011GB107001. LLNL-PRES-635587

Principal Results

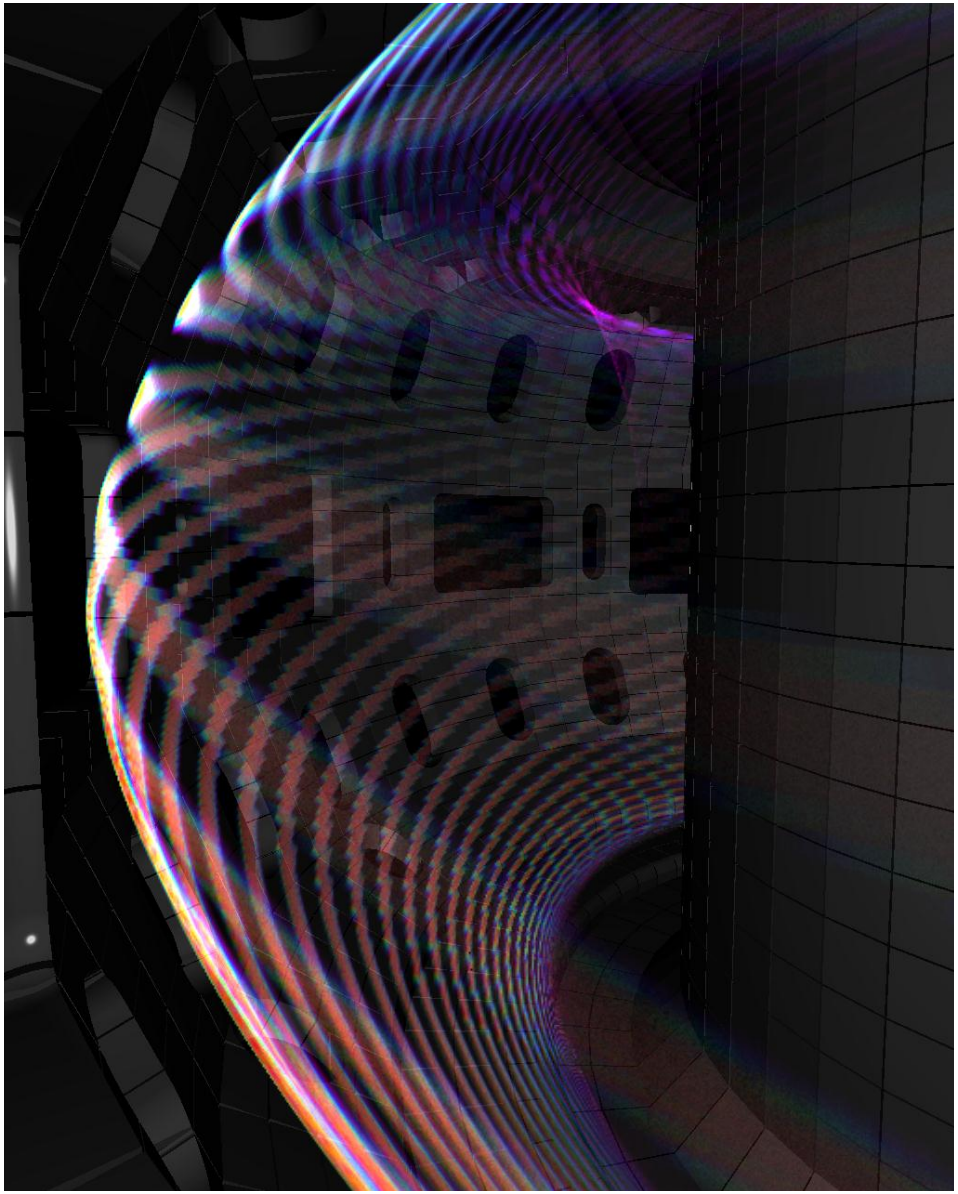

- A suite of two-fluid models has been implemented in BOUT++ for
  - ✓ different ELM regimes and fluid turbulence
- A suite of gyro-fluid models is under development for
  - ✓ pedestal turbulence and transport
- Kinetic effect of parallel diffusion implemented
  - ✓ flux limited expressions for $\chi_{||j}$
  - ✓ nonlocal GLF models for $q_{||j}$
- We find that both pressure gradient α and pedestal density n can control the transition from large ELMs to small ELMs.
  - ✓ Small elms can be either resistive or ideal P-B modes
  - ✓ Elm size dependence on density is due to ion diamagnetic stabilization, not due to collisionality

BOUT++: A framework for nonlinear twofluid and gyrofluid simulations ELMs and turbulence

- **Different twofluid and gyrofluid models are developed under BOUT++ framework for ELM and turbulence simulations**

Twofluid	Gyrofluid	Physics
3-field $(\varpi, P, A_\parallel)$	**1+0** $(n_{iG}, n_e, A_\parallel)$	**Peeling-ballooning mode**
4-field $(\varpi, P, A_\parallel, V_\parallel)$	**2+0** $(n_{iG}, n_e, A_\parallel, V_\parallel)$	**+ acoustic wave**
5-field $(\varpi, n_i, A_\parallel, T_i, T_e)$		**+ Thermal transport no acoustic wave**
6-field $(\varpi, n_i, A_\parallel, V_\parallel, T_i, T_e)$ **Braginskii equations**	**3+1** $(n_{iG}, n_e, A_\parallel, V_\parallel, T_{i\perp}, T_{i\parallel}, T_e)$ Snyder+Hammett’s model	**+ additional drift wave instabilities + Thermal transport**

4-field model agrees well with 3-field for both ideal and resistive ballooning modes

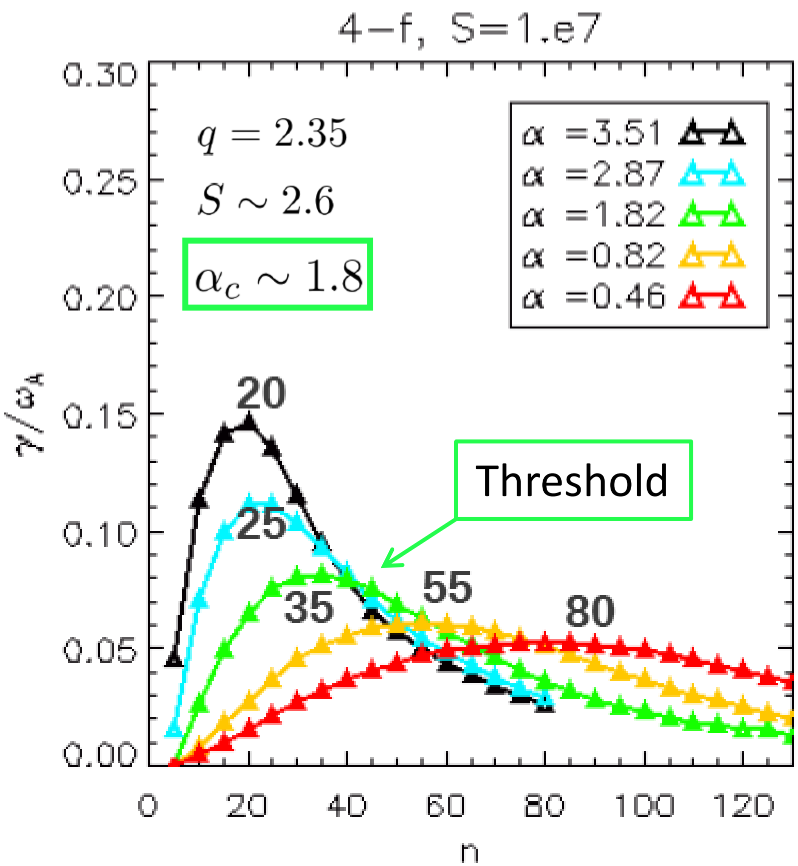

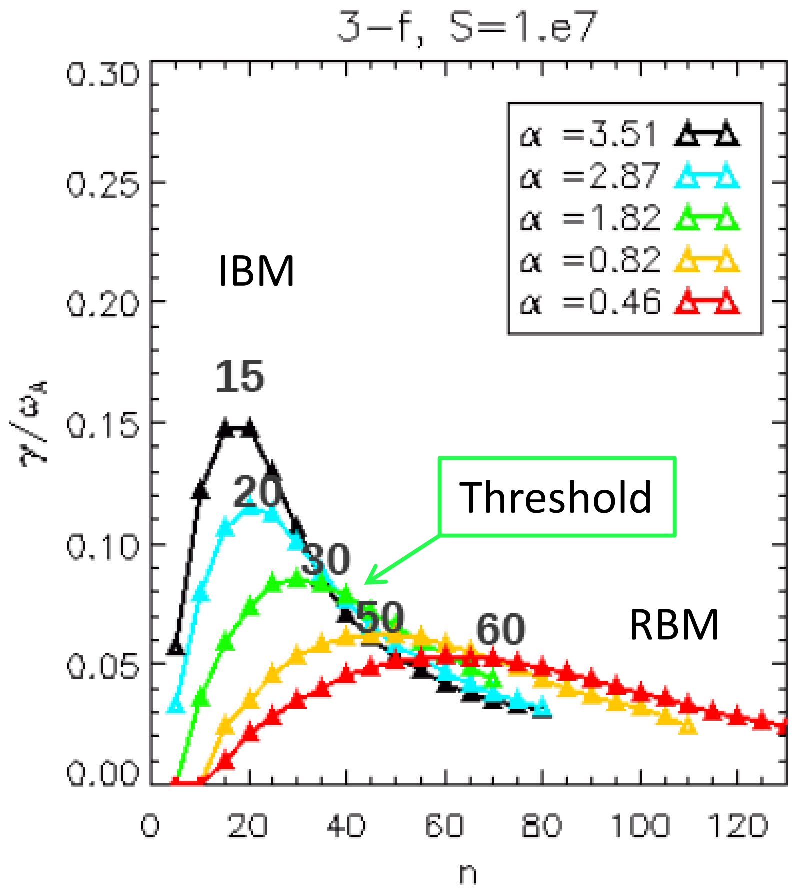

- α_c value from eigenvalue solver agrees with BOUT simulation.
- Non-ideal effects are consistent in both models
  - ✓ diamagnetic stabilization
  - ✓ resistive mode with $\alpha < \alpha_c$
  - ✓ increase n of maximum growth rate with decrease of α

Six-field two-fluid models have been developed in BOUT++ for ELMs and turbulence simulations

- **Six-field (ϖ, n_i, T_i, T_e, $A_{||}$, $V_{||}$):**
  based on Braginskii equations, the density, momentum and energy of ions and electrons are described in drift ordering*.
  - ✓ **nonlinear || thermal diffusivities**
  - ✓ **nonlinear resistivity**
  - ✓ **additional drift wave instabilities**

Lundquist number profile

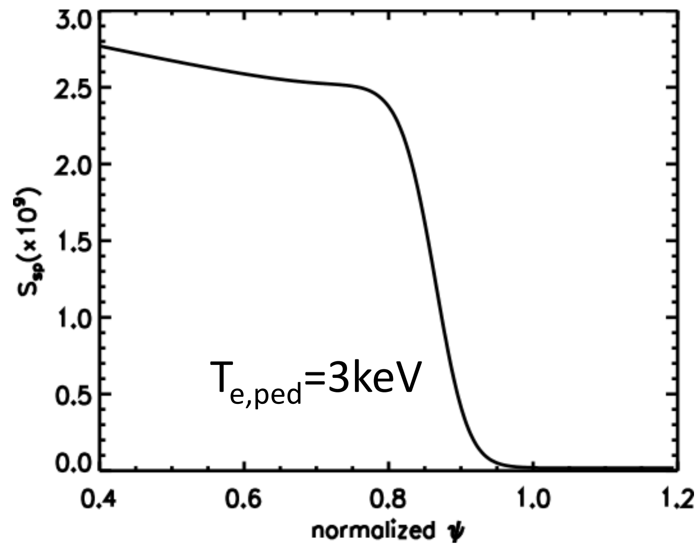

- **|| thermal diffusivities with flux limited expressions reduce ELM size:**

$$\chi_{||i} = 3.9\frac{v_{th,i}^2}{\nu_i} \quad \chi_{||e} = 3.2\frac{v_{th,e}^2}{\nu_e} \quad \chi_{fl,j} = v_{th,j}q_{95}R_0$$

Flux limited expression:

$$\chi_{||j}^{e} = \left(\frac{1}{\chi_{||j}} + \frac{1}{\chi_{flj}}\right)^{-1}$$

- **GLF models for $\chi_{||j}$ are under development**

Electron parallel thermal diffusivity profile

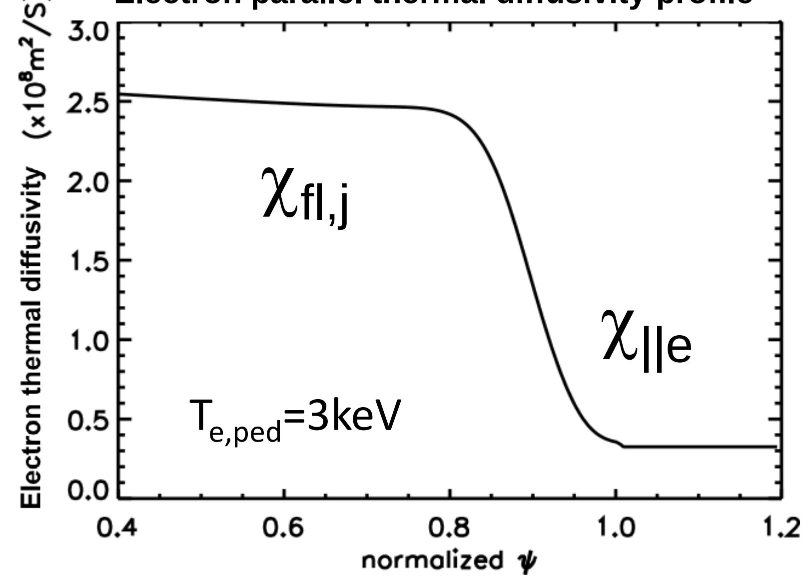

*X. Q. Xu et al., Commun. Comput. Phys. 4, 949 (2008).

The 3-field 2-fluid model is good enough to simulate P-B stability and early phase of ELM crashes for large ELMs, additional physics from multi-field contributes less than 8.3% corrections

- **Fundamental physics in ELMs:**
  - ✓ Peeling-Ballooning instability
  - ✓ Ion diamagnetic stabilization
    - → kinetic effect
  - ✓ Resistivity and hyper-resistivity
    - → reconnection

- **Additional physics:**
  - Ion acoustic waves
  - || thermal conductivities
  - Hall effect
  - Compressibility
  - Electron-ion friction

BUT

change the peak linear growth rate less than 8.3%

- ✓ **Power loss via separate ion & electron channels**
- ✓ **Power depositions on PFCs.**
- ✓ **Turbulence and transport**

$$
\begin{aligned}
\frac{\partial}{\partial t}\varpi &= -\left(\frac{1}{B_0}\boldsymbol{b}\times\boldsymbol{\nabla}_\perp\Phi + V_{\|e}\boldsymbol{b}\right)\cdot\boldsymbol{\nabla}\varpi \\
&\quad + B^2\nabla_\|\left(\frac{J_\|}{B}\right) + 2\boldsymbol{b}\times\boldsymbol{\kappa}\cdot\boldsymbol{\nabla}P \\
&\quad -\frac{1}{2\Omega_i}\left[\frac{1}{B}\boldsymbol{b}_0\times\boldsymbol{\nabla}P_i\cdot\boldsymbol{\nabla}\left(\nabla_\perp^2\Phi\right) - Z_ieB\boldsymbol{b}\times\boldsymbol{\nabla}n_i\cdot\boldsymbol{\nabla}\left(\frac{\nabla\Phi}{B}\right)^2 + Z_ieB\boldsymbol{b}\times\boldsymbol{\nabla}n_i\cdot\boldsymbol{\nabla}\left(\frac{\nabla_\|\Phi}{B}\right)^2\right] \\
&\quad +\frac{1}{2\Omega_i}\left[\frac{1}{B}\boldsymbol{b}_0\times\boldsymbol{\nabla}\Phi\cdot\boldsymbol{\nabla}\left(\nabla_\perp^2P_i\right) - \nabla_\perp^2\left(\frac{1}{B}\boldsymbol{b}_0\times\boldsymbol{\nabla}\Phi\cdot\boldsymbol{\nabla}P_i\right)\right],
\end{aligned}
$$

$$
\begin{aligned}
\frac{\partial}{\partial t}n_i &= -\left(\frac{1}{B_0}\boldsymbol{b}\times\boldsymbol{\nabla}_\perp\Phi + V_{\|i}\boldsymbol{b}\right)\cdot\nabla n_i \\
&\quad -\frac{2n_i}{B}\boldsymbol{b}\times\boldsymbol{\kappa}\cdot\boldsymbol{\nabla}_\perp\Phi - \frac{2}{Z_ieB}\boldsymbol{b}\times\boldsymbol{\kappa}\cdot\boldsymbol{\nabla}_\perp P - n_iB\nabla_\|\left(\frac{V_{\|i}}{B}\right)
\end{aligned}
$$

$$
\frac{\partial}{\partial t}A_\| = -\nabla_\|\phi - \eta J_{\|1} + \frac{1}{en_e}\nabla_\|P_e + \frac{0.71k_B}{e}\nabla_\|T_e.
$$

$$
\frac{\partial}{\partial t}V_{\|i} = -\left(\frac{1}{B_0}\boldsymbol{b}\times\boldsymbol{\nabla}_\perp\Phi + V_{\|i}\boldsymbol{b}\right)\cdot\boldsymbol{\nabla}V_{\|i} - \frac{1}{m_in_i}\boldsymbol{b}\cdot\boldsymbol{\nabla}P,
$$

$$
\begin{aligned}
\frac{\partial}{\partial t}T_i &= -\left(\frac{1}{B_0}\boldsymbol{b}\times\boldsymbol{\nabla}_\perp\Phi + V_{\|i}\boldsymbol{b}\right)\cdot\boldsymbol{\nabla}T_i \\
&\quad -\frac{2}{3}T_i\left[\left(\frac{2}{B}\boldsymbol{b}\times\boldsymbol{\kappa}\right)\cdot\left(\boldsymbol{\nabla}\Phi + \frac{1}{Z_ien_i}\boldsymbol{\nabla}P_i + \frac{5}{2}\frac{k_B}{Z_ie}\boldsymbol{\nabla}T_i\right) + B\nabla_\|\left(\frac{V_{\|i}}{B}\right)\right] \\
&\quad +\frac{2}{3n_ik_B}\nabla_\|\left(\kappa_{\|i}\nabla_\|T_i\right) + \frac{2}{3n_ik_B}\nabla_\perp\left(\kappa_{\perp i}\nabla_\perp T_i\right) \\
&\quad +\frac{2m_e}{m_i}\frac{Z_i}{\tau_e}\left(T_e - T_i\right)
\end{aligned}
$$

$$
\begin{aligned}
\frac{\partial}{\partial t}T_e &= -\left(\frac{1}{B_0}\boldsymbol{b}\times\boldsymbol{\nabla}_\perp\Phi + V_{\|e}\boldsymbol{b}\right)\cdot\boldsymbol{\nabla}T_e \\
&\quad -\frac{2}{3}T_e\left[\left(\frac{2}{B}\boldsymbol{b}\times\boldsymbol{\kappa}\right)\cdot\left(\boldsymbol{\nabla}\Phi - \frac{1}{en_e}\boldsymbol{\nabla}P_e - \frac{5}{2}\frac{k_B}{e}\boldsymbol{\nabla}T_e\right) + B\nabla_\|\left(\frac{V_{\|e}}{B}\right)\right] \\
&\quad -0.71\frac{2T_e}{3en_e}B\nabla_\|\left(\frac{J_\|}{B}\right) \\
&\quad +\frac{2}{3n_ek_B}\nabla_\|\left(\kappa_{\|e}\nabla_\|T_e\right) + \frac{2}{3n_ek_B}\nabla_\|\left(\kappa_{\perp e}\nabla_\perp T_e\right) \\
&\quad -\frac{2m_e}{m_i}\frac{1}{\tau_e}\left(T_e - T_i\right) + \frac{2}{3n_ek_B}\eta_\|J_\|^2
\end{aligned}
$$

6-field model is qualitatively consistent with 3-field and 5-field models on large ELMs

Equilibrium 1: smaller pressure gradient
Equilibrium 2: more Peeling-Ballooning unstable

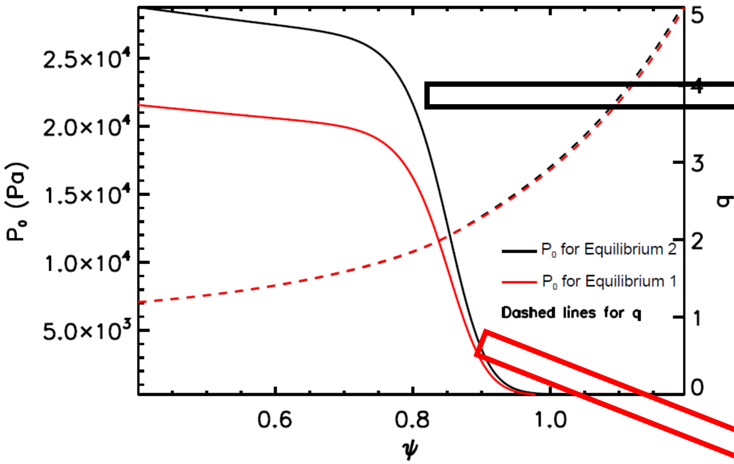

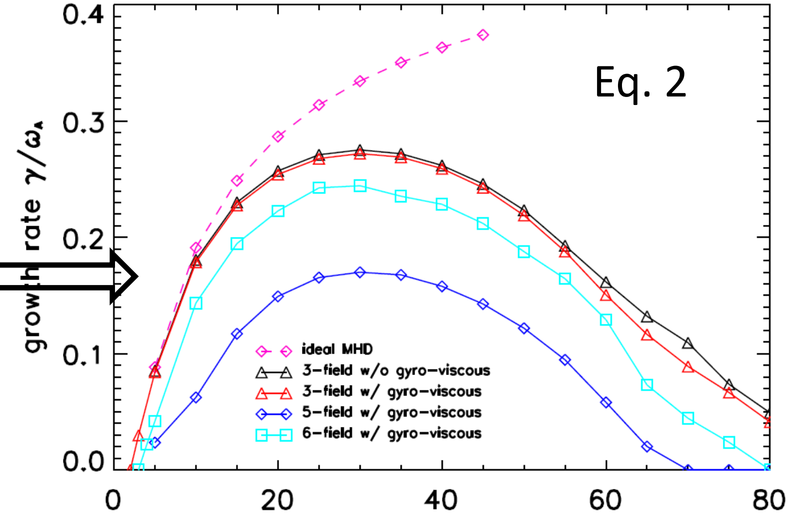

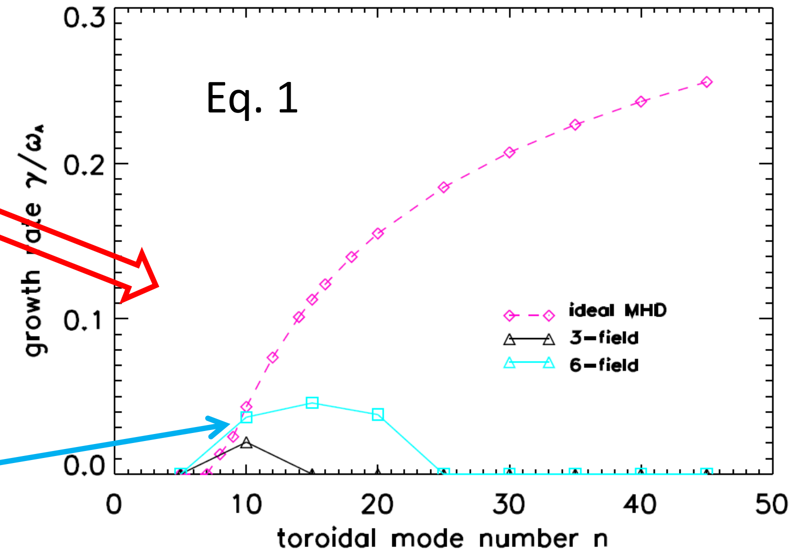

The instabilities are the same in 6-field, but the additional physics drives the mode mores unstable

6-field model is qualitative consistent with 3-field and 5-field models on large ELMs

Equilibrium 1: smaller pressure gradient
Equilibrium 2: more Peeling-Ballooning unstable

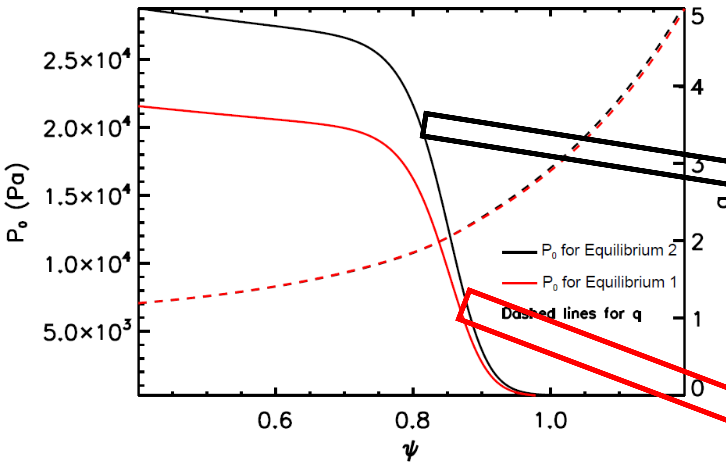

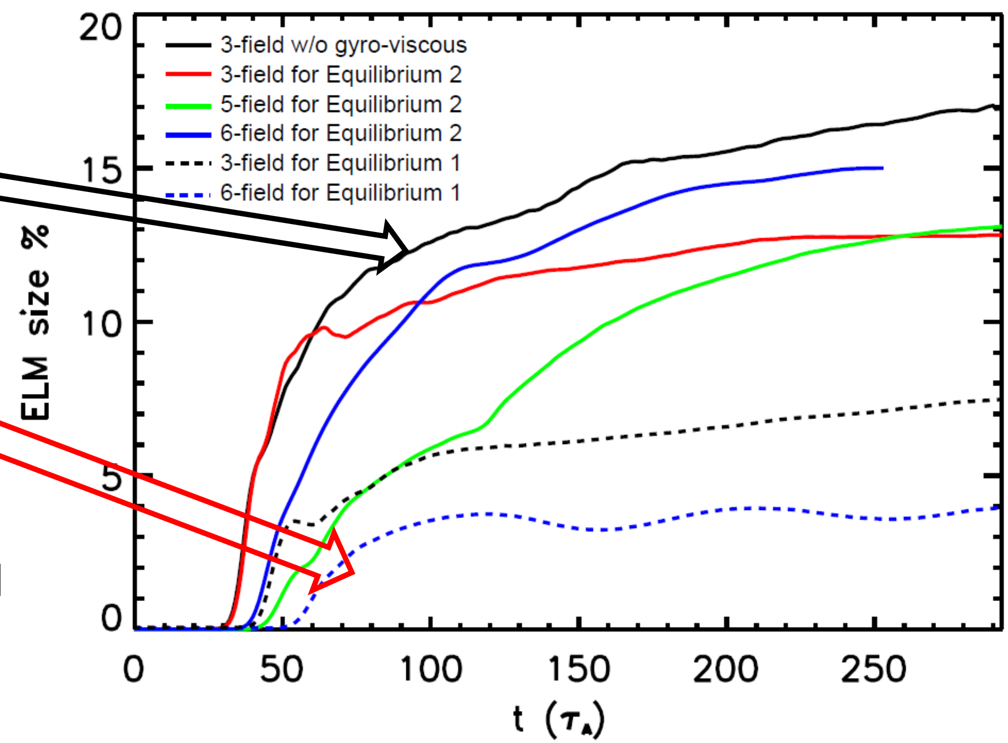

- For large ELMs, 3-field model is good enough.
- For small ELMs, 6-field model is necessary to simulate
  - Turbulence
  - Transport
  - Energy deposition on PFCs

* Definition of ELM size:

$$\Delta_{ELM}^{th} = \frac{\Delta W_{ped}}{W_{ped}} = \frac{\langle \int_{R_{in}}^{R_{out}} \oint dR d\theta (P_0 - \langle P \rangle_\zeta) \rangle_t}{\int_{R_{in}}^{R_{out}} \oint dR d\theta P_0},$$

For the same equilibrium
with same pressure and current profiles,
but with different density and temperature profiles

Pedestal pressure and current alone are not enough to determine the transition

For same P_0, $J_{||0}$ and geometry, increasing densities leads to less ion diamagnetic stabilization and more high-n unstable modes

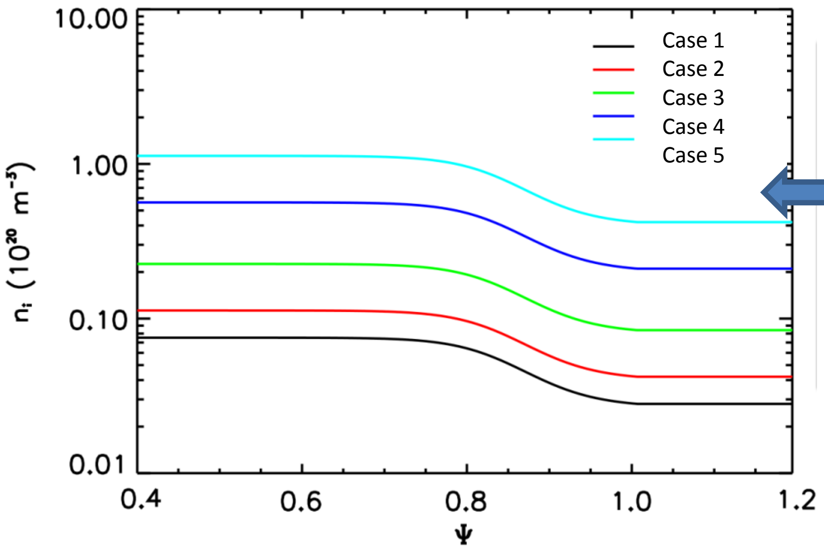

Five density profiles with the same pressure and current.

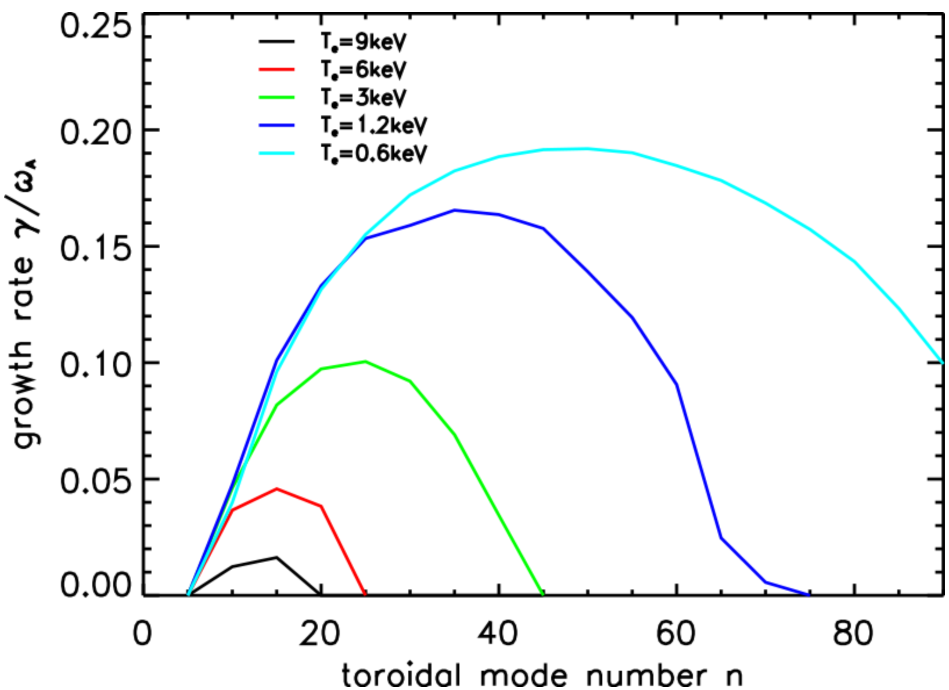

- Case 3, 4 and 5: large ELMs
- Case 2: small ELMs
- Case 1: very small resistive ballooning modes, turbulence

Pedestal pressure and current alone are not enough to determine the transition

For same P_0, $J_{||0}$ and geometry, the scan of 5 different densities shows the transition from large to small ELMs, due to ion diamagnetic stabilization

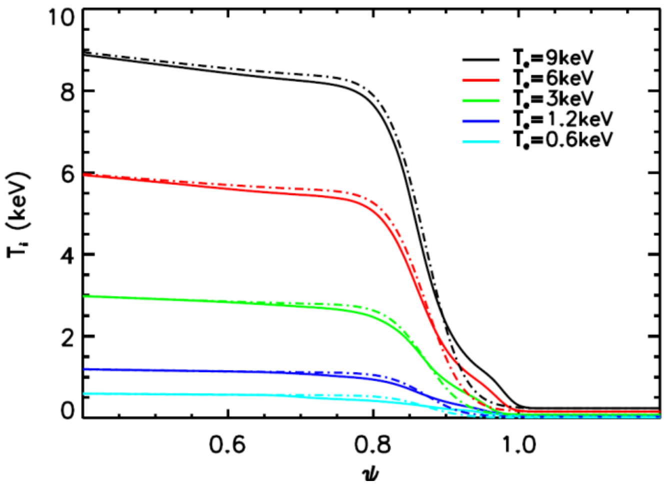

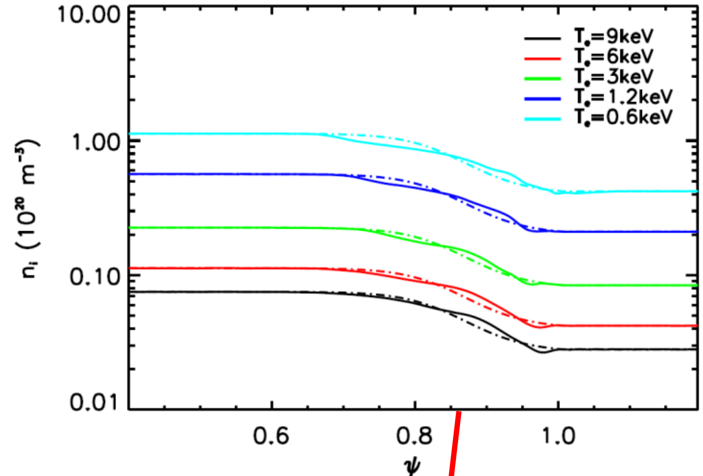

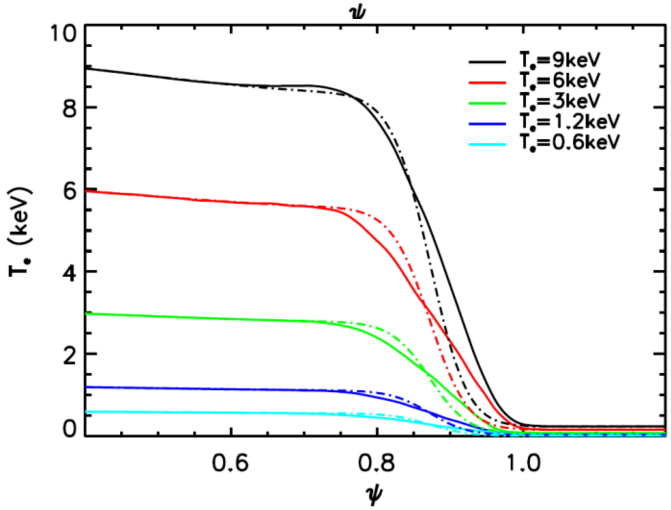

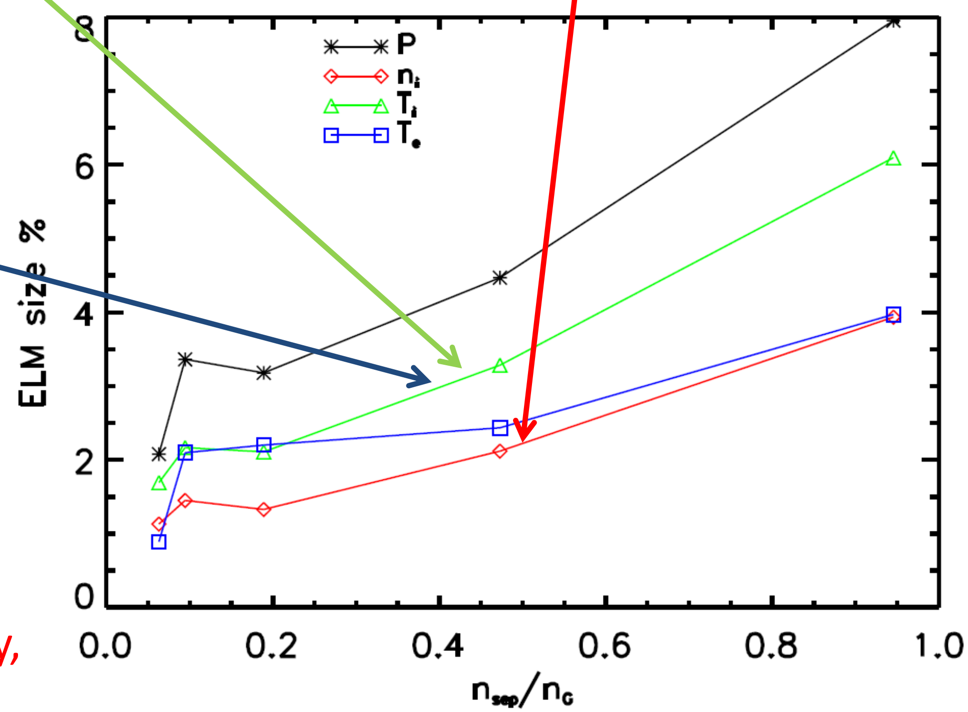

- Ion temperature contributes most to total ELM size
- Elm size depends on the pedestal density, not collisionality

The flux limited expressions of parallel thermal diffusivities show no collisionality dependence, even in the SOL

Thermal diffusivities with flux limited expressions suppress the increase of ELM size:

$$\chi_{\parallel i}^{SP} = 3.9\frac{v_{th,i}^2}{\nu_i}, \qquad \chi_{\parallel e}^{SP} = 3.2\frac{v_{th,e}^2}{\nu_e}$$

$$\chi_{fs,j} = v_{th,j} q R_0$$

Flux limited expression:

$$\chi_{\parallel j}^{eff} = \frac{\chi_{\parallel j}^{SP}\chi_{fs,j}}{\chi_{\parallel j}^{SP} + \chi_{fs,j}}$$

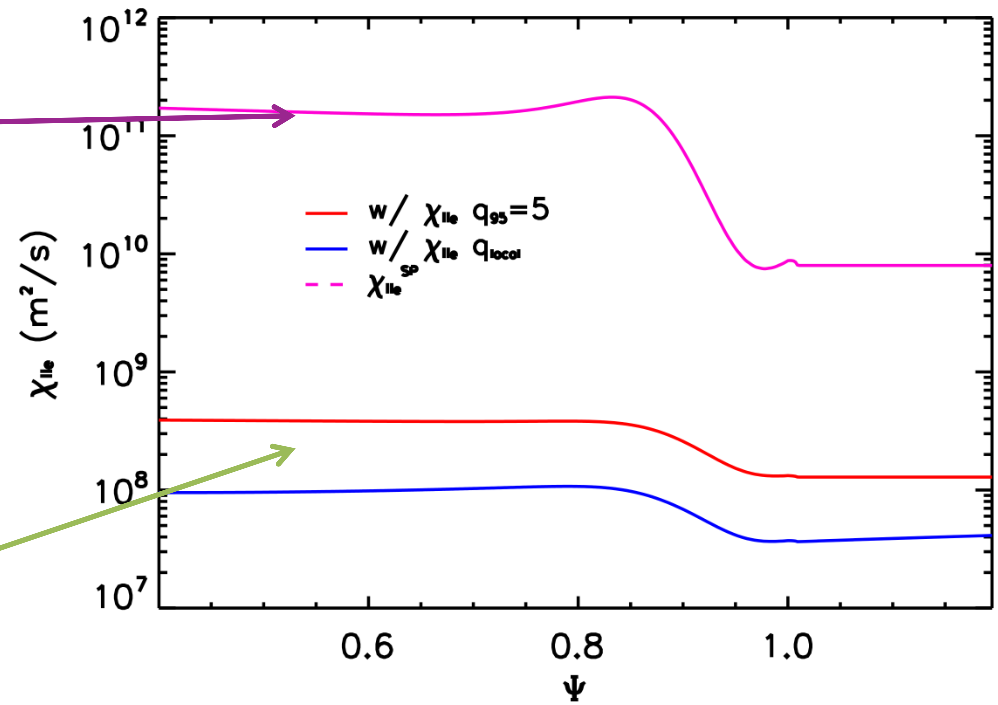

Two different free-streaming expressions are used to verify the effects of $\chi_{||j}$:

Red: q=5

Blue: q profile with q_{max} <5

More real experimental data needed to confirm this conclusion

For the same equilibrium
with different pressure and current profiles,
but with the same density

6-field simulations show that smaller pedestal height leads to smaller ELMs, due to smaller α

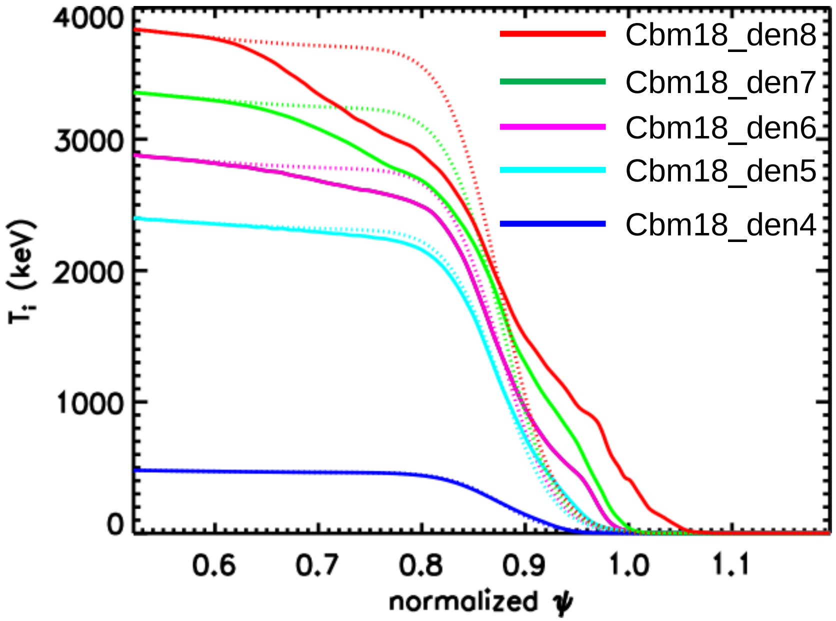

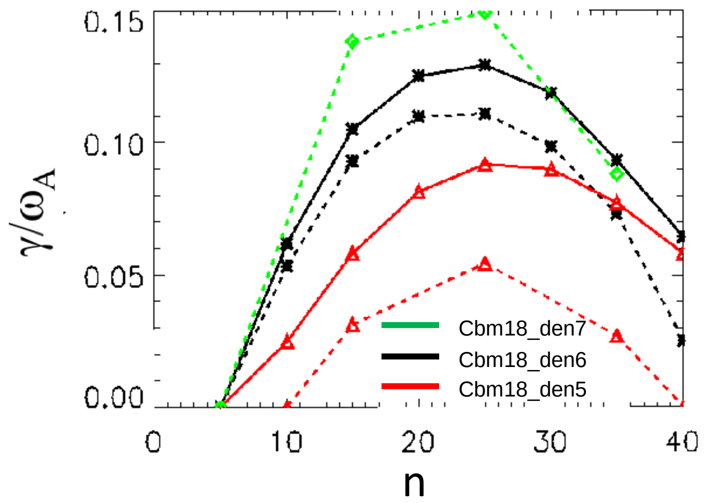

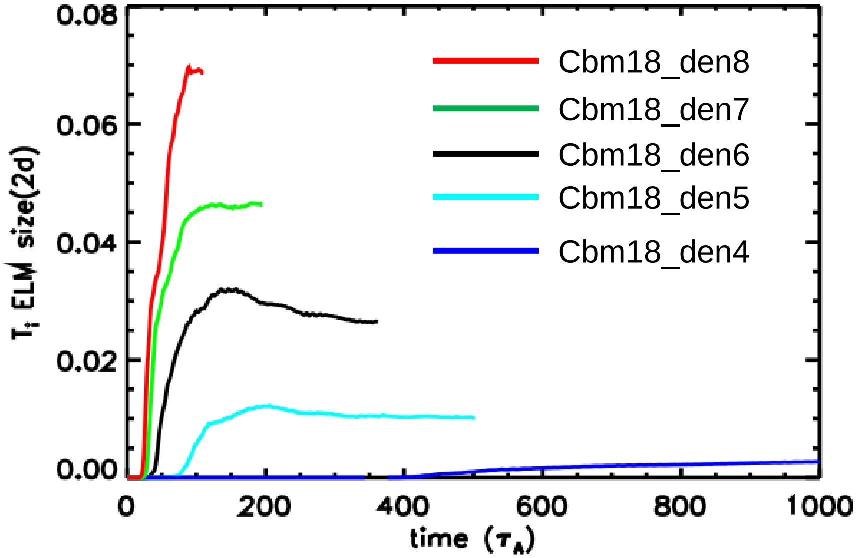

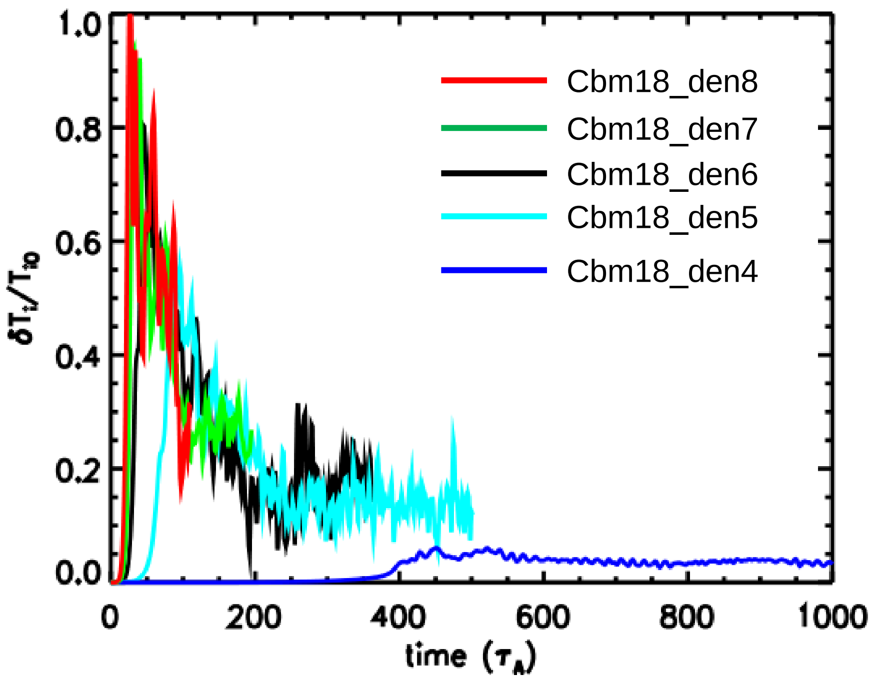

6-field simulations show the separation of particle and energy transport channels

Six-field simulations show that most energy lost via ion channel during an ELM event, followed by electron channel and then by particle channel

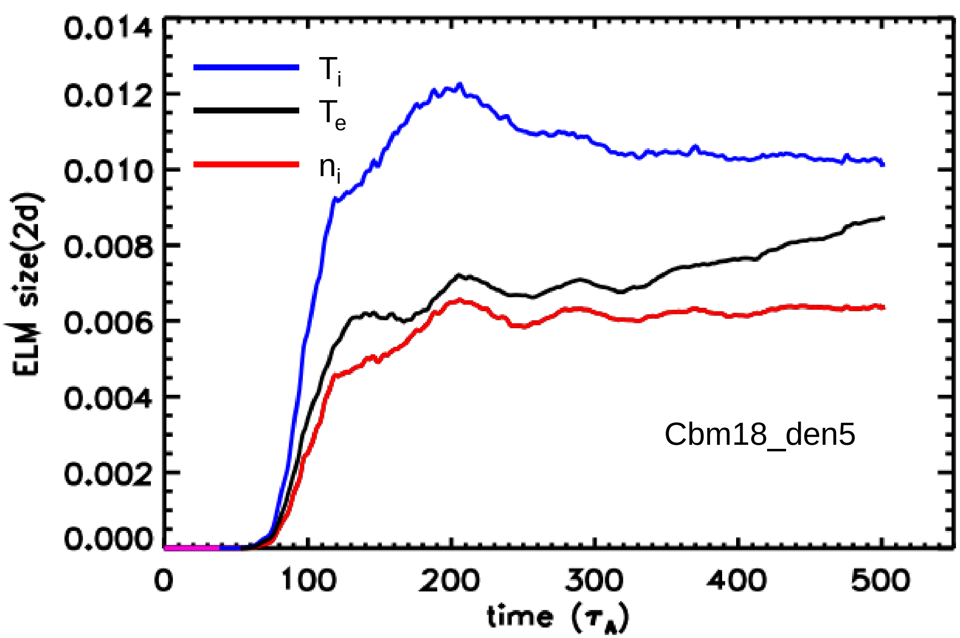

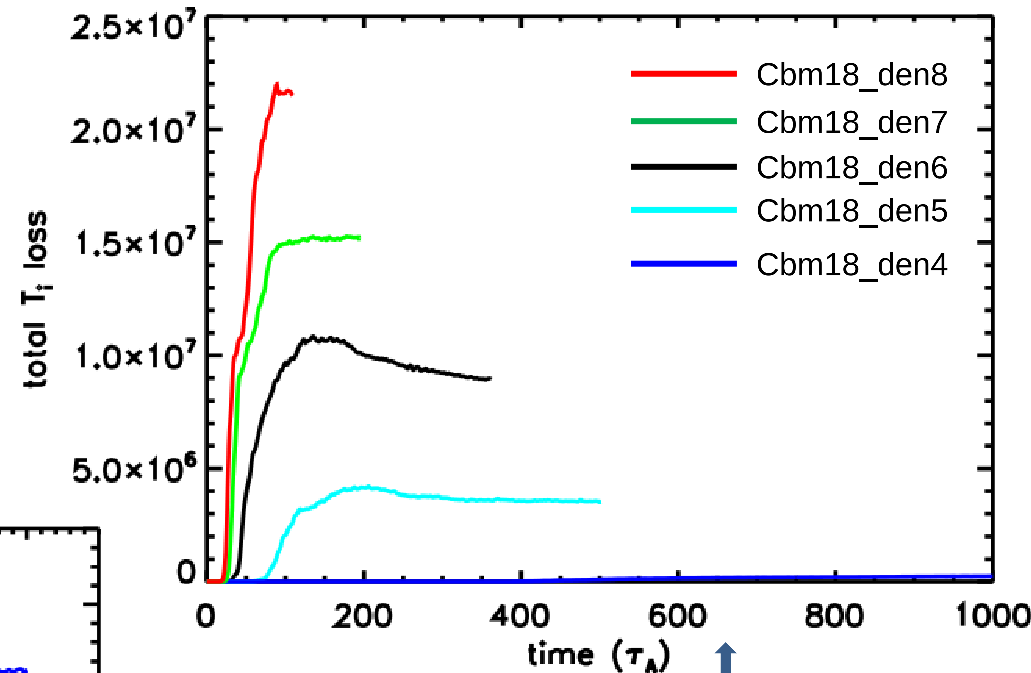

The total energy lost via ion channel during an ELM event

* Definition of ELM size:

$$\Delta_{ELM}^{th} = \frac{\Delta W_{ped}}{W_{ped}} = \frac{\langle \int_{R_{in}}^{R_{out}} \oint dR d\theta (P_0 - \langle P \rangle_\zeta) \rangle_t}{\int_{R_{in}}^{R_{out}} \oint dR d\theta P_0},$$

Landau damping has stronger stabilizing effect on P-B modes than flux limited expression

- **Flux limited thermal conductivity**

$$q_{\parallel i} = -\kappa_{\parallel i} \nabla_{\parallel} k_B T_i$$
$$q_{\parallel e} = -\kappa_{\parallel e} \nabla_{\parallel} k_B T_e$$

Where

$$\kappa_{\parallel i} = \left({\kappa_{\parallel i}^{SH}}^{-1} + {\kappa_{\parallel i}^{FS}}^{-1} \right)^{-1}$$
$$\kappa_{\parallel e} = \left({\kappa_{\parallel e}^{SH}}^{-1} + {\kappa_{\parallel e}^{FS}}^{-1} \right)^{-1}$$
$$\kappa_{\parallel i}^{SH} = 3.9 n_i v_{th,i}^2 / \nu_i$$
$$\kappa_{\parallel e}^{SH} = 3.2 n_e v_{th,e}^2 / \nu_e$$
$$\kappa_{\parallel j}^{FS} = n_j v_{th,j} q R_0$$

- **Landau damping closure ***

$$\tilde{q}_{\parallel,\alpha} = -n_0 \sqrt{\frac{8}{\pi}} v_{t\parallel} \frac{i k_{\parallel} k_B \tilde{T}_{\alpha}}{|k_{\parallel}|}, \alpha = i, e$$

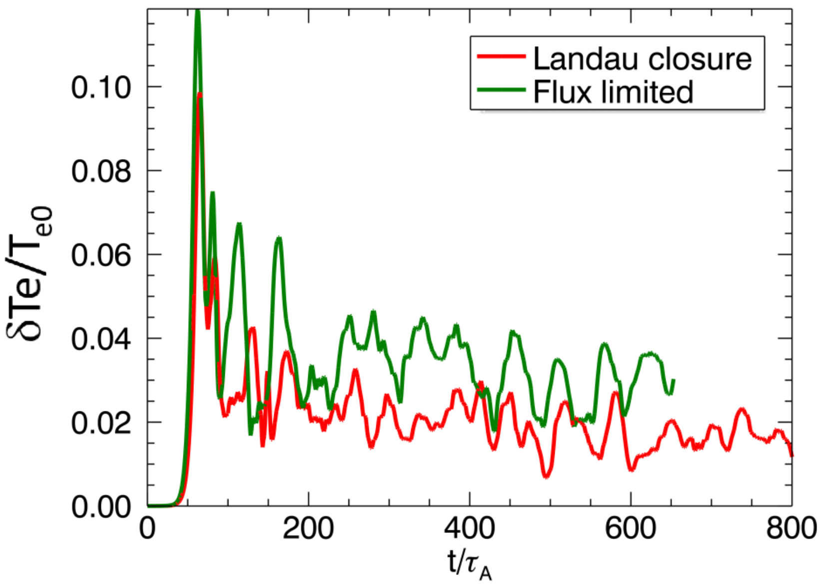

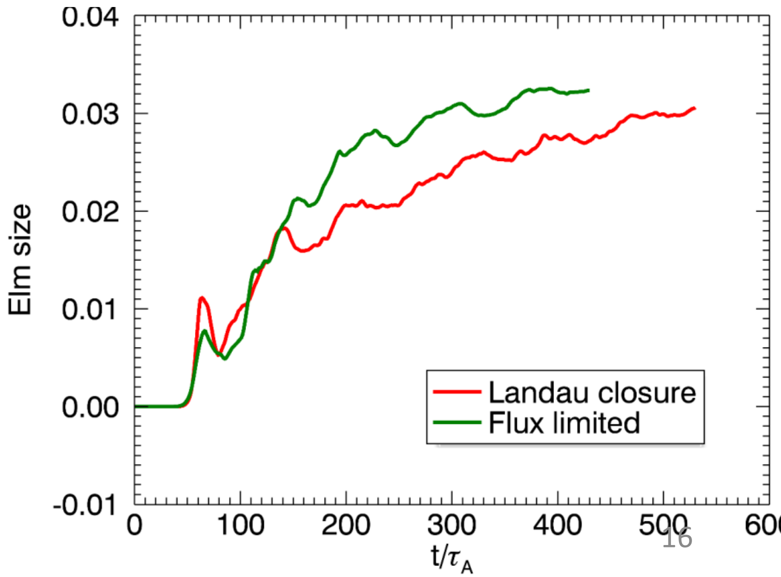

Landau damping and flux limited heat flux has no damping effect on rational surface due to $k_\parallel = 0$ as expected

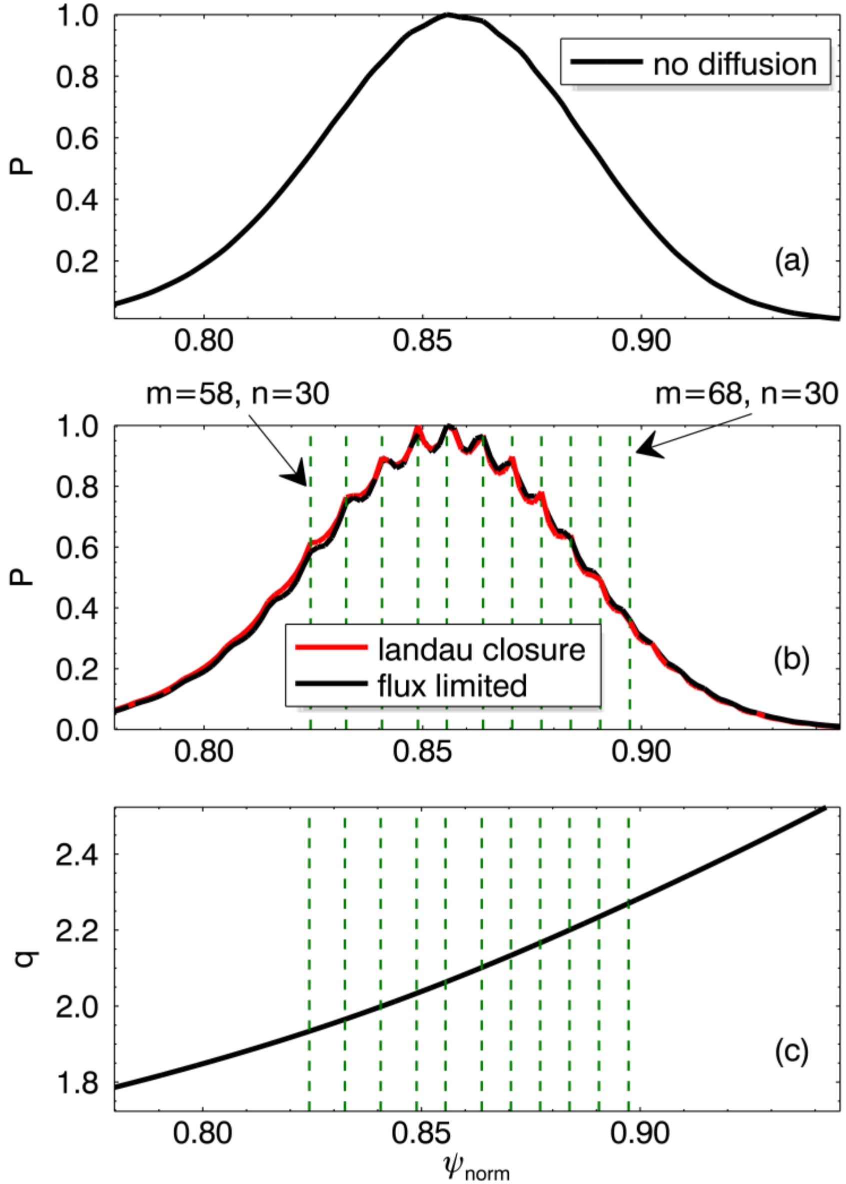

- Radial mode structure:
  - Without parallel diffusion: smooth;
  - With Landau damping or flux limited heat flux: peaked at rational surfaces.

	Rational surface	Non-rational surface
Instability	Strong	Weak
Parallel damping	Weak	Strong

✓ The dmismatch between instability and parallel damping reduces the efficiency of parallel damping stabilization on peeling-ballooning modes.

BOUT++ global GLF model agrees well with gyrokinetic results

- **BOUT++ using Beer's 3+1 model agrees well with gyrokinetic results.**
- **Non-Fourier method for Landau damping shows good agreement with Fourier method.**

Implemented in the BOUT++

- ✓ **Padé approximation for the modified Bessel functions**
- ✓ **Landau damping**
- ✓ **Toroidal resonance**
- **Zonal flow closure in progress**
- **Nonlinear benchmark underway**

Developing the GLF models

- to behave well at large perturbations
- for second-order-accurate closures

$\Rightarrow$ **Self-consistent global nonlinear kinetic ITG/KBM simulations at pedestal and collisional drift ballooning mode across the separatrix in the SOL**

Cyclone base case

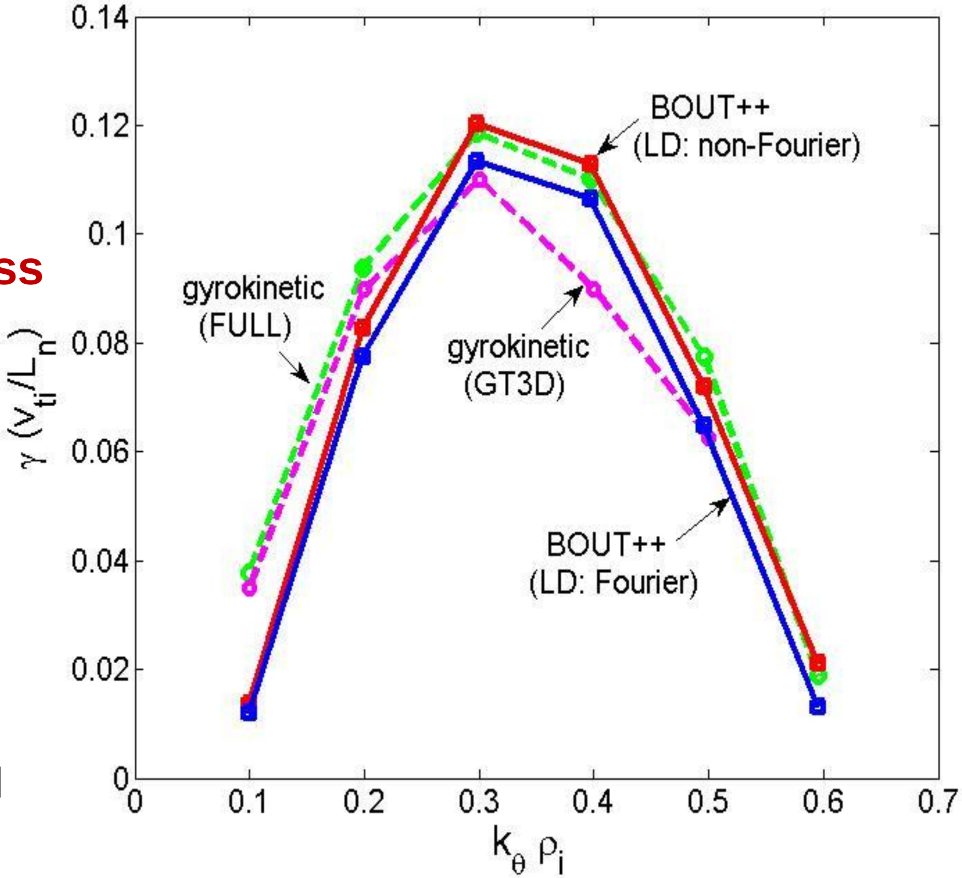

Principal Results

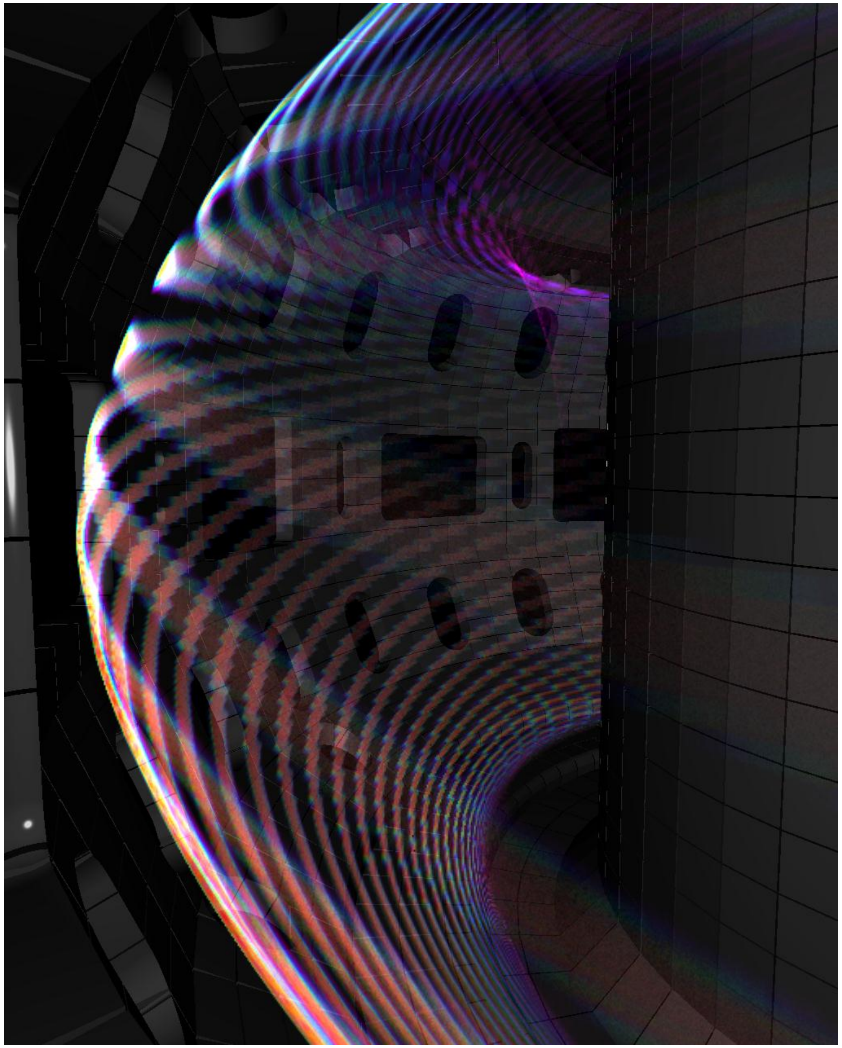

- A suite of two-fluid models has been implemented in BOUT++ for
  - ✓ all ELM regimes and fluid turbulence
- A suite of gyro-fluid models is under development for
  - ✓ pedestal turbulence and transport
- We find that both pressure gradient α and pedestal density n can control the transition from large ELMs to small ELMs.
  - ✓ Small elms can be either resistive or ideal P-B modes
  - ✓ Elm size dependence on density is due to ion diamagnetic stabilization, not due to collisionality
  - ✓ The flux limited expressions of parallel thermal diffusivities show no collisionality dependence, even in the SOL
- A decrease of the ELM size with density is a natural consequence for ballooning modes.

Remaining questions

- **Type-I ELMs should be mainly dominated by peeling modes**
  - ✓ **will conduct simulations for nonlinear peeling modes**

- **Ideal ballooning modes (IBMs) yield wrong elm size dependence with density for type-I ELMs**
  - **a puzzle to be solved if IBMs are responsible to type-I ELMs**

- **Type-III ELMs should be mainly dominated by ballooning modes which give consistent elm size dependence with density**